IJE TRANSACTIONS A: Basics Vol. 34, No. 7, (July 2021) 1632-1643

International Journal of Engineering

Journal Homepage: www.ije.ir

Performance of Reinforced Concrete Shear Wall Equipped with an Innovative Hybrid Damper

M. Abedi, M. Jalali*, J. Shafaei

Faculty of Civil engineering, Shahrood University of Technology, Shahrood, Iran

PAPER INFO

Paper history:
Received 26 April 2021
Received in revised form 18 May 2021
Accepted 19 May 2021

Keywords:
Residual Displacement
Shape Memory Alloy
Concrete Shear Wall
Hybrid Damper
Numerical Modelling
Super-elastic Behaviour

ABSTRACT

The performance of simultaneous application of steel cantilever damper and Shape Memory Alloy (SMA) rods in the reinforced concrete (RC) shear wall was investigated. In this regard, the critical numerical validation of three full-scale experimental models were distinctly performed and the results were analyzed. Various aspects of numerical modelling, including material modelling assumptions, behavioural models, elements, and solution methods were compared with experimental results. Specimens considering SMA rods as well as steel cantilever damper were numerically investigated. The results illustrated that with increasing the SMA rod angle, the maximum force was decreased, and the residual displacement and dissipated energy was improved. Also, comparing the specimen results without the SMA rods and the specimen with the SMA rods showed that despite the positive effect of the SMA rods, which leads to an increase in maximum force and reduction of residual displacement, the dissipated energy was decreased.

doi: *10.5829/ije.2021.34.07a.08*

1. INTRODUCTION

The use of steel dampers is one of the passive control methods against earthquakes, which has expanded due to economic and production advantages. In this method, by damper inelastic behaviour, energy is dissipated, and by concentrating the damage in it, damage to other members is prevented. It is also easy to replace this type of damper [1]. In addition to structural damage that leads to the unusability of the structure, residual displacement also causes residents' insecurity.

Due to shaped memory alloy features, researchers have studied their performance in the structure in recent years. The first known example of using a shaped memory alloy in a structure dates back to the repair of the bell tower of the Church of San Georgia in the Trignano region of Italy. The tower was damaged by a 4.8 magnitude earthquake in 1996. To repair, four vertical prestressed steel bars with SMA were placed in the inner corners to increase the structure's flexural strength. SMA machine was made of 60 wires with a diameter of 1 mm and a length of 300 mm. In 2000, the structure was hit by a 4.5 magnitude earthquake; observations showed that the structure was not damaged. In another similar project, Croci retrofit a building damaged by the 1997 earthquake in Assisi, Italy, with super-elastic SMAs [2]. DesRoches et al. [3] Studied the properties of wires and rods made of shape memory alloys composed of nickel and titanium alloys to determine the effects of rod size, loading history, and loading rate on the amount of energy dissipation, self-centering ability, and stress of shift phase. Sayyaadi and Zakerzadeh [4] also examined SMA wires. Kim et al. [5] suggested a type of steel damper to improve the seismic of existing structures. The damper was fixed at one end and free at another end, resulting in behaviour like a cantilever. Lu et al. [6] Examined three systems of structures resistant to lateral forces. They conducted their research on a self-centering concrete frame exposed to a vibrating table, quasi-static loading on a concrete shear wall equipped with self-centering coupler beams, and a concrete shear wall equipped with replaceable members at the foot of the wall. All three structural systems performed effectively against lateral force. Kim et al. [7] examined steel cantilever dampers

*Corresponding Author Institutional Email: mjalali@sharoodut.ac.ir
(M. Jalali)

Please cite this article as: M. Abedi, M. Jalali, J. Shafaei Performance of Reinforced Concrete Shear Wall Equipped with an Innovative Hybrid Damper, International Journal of Engineering, Transactions A: Basics Vol. 34, No. 7, (2021) 1632-1643

under different conditions. The results showed that the damper in a small displacement yielded, and the behaviour of stable hysteresis and the loops' shape is close to a parallelogram, which indicates its high energy dissipation capacity. Ahn et al. [8] tested a concrete shear wall equipped with a steel cantilever damper and an isolator under quasi-static loading. In this study, four specimens with different loading conditions were used. One of the specimens was drifted at 2%, and the other three specimens were loaded in two stages. The results showed that with increasing the initial load drift, the deformation of the steel cantilever damper plastic increases, and the total energy dissipation in the second stage is significantly reduced; however, no severe damage was observed in the wall. Naeem et al. [9] built a hybrid energy dissipator by combining a memory alloy rod with a slotted steel plate. The results showed that the maximum drift between the floor and the displacement of the roof of the model structure equipped with a bar made of memory alloy is significantly reduced. Puentes and Palermo [10] examined braced concrete shear walls with and without steel bracing and SMA. The results showed that in the shear wall model equipped with bracing, resistance, energy dissipation, and displacement recovery increased, stiffness and strength degradation decreased. Liu and Jiang [11] tried to focus possible damage on the replaceable members at the corners of the concrete shear wall. The results showed that lateral load-bearing capacity, ductility, and energy dissipation capacity increased. Liu and Jiang [12] modelled a concrete shear wall with replaceable members at the corners of the wall's foot with different compressive axial force ratios in ABAQUS software. The results showed that walls equipped with replaceable members with a larger axial load ratio, larger load capacity, and larger deformation. Chen et al. [13] Examined a concrete shear wall equipped with a coupler beam and replaceable members at the wall's foot using numerical modelling. In general, shear walls equipped with replaceable members have been shown to dissipate energy better. Puentes and Palermo [14] developed a bracing system consisting of a nickel-titanium super-elastic memory alloy under tensile force to improve the fat shear concrete wall. This study focused on 1.3-scale walls representing concrete shear walls before the 1970s that are prone to shear slippage and oblique cracking. The results showed that walls equipped with shaped memory alloy bracing improved seismic performance, including lateral resistance capacity, ductility, energy dissipation, and displacement recovery. Wang and Zhu [15] explored the possibility of using super-elastic memory alloy bars to access the self-centering reinforced concrete walls. In this study, modelling and nonlinear analysis were performed using the OpenSees finite element program and compared with laboratory results. The results show that although the self-centered reinforced concrete walls dissipation relatively less energy through hysteresis loops, almost no residual deformation remains after cyclic loading with a maximum drift of 2.5%. NourEldin et al. [16] used a slotted steel damper equipped with a shaped memory rod in a steel frame with eccentric bracing and analyzed the fragility and cost-effectiveness of the life cycle. The results showed that the frame equipped with a hybrid damper had a lower seismic response than the frame with a slotted damper due to the increase in seismic performance due to the extra stiffness, energy dissipation, and self-centering ability provided by the SMA rod. The results also showed that the life cycle cost of frames equipped with hybrid dampers was lower compared to frames without slotted dampers, although the initial costs of hybrid dampers were higher than those of slotted dampers. Wang et al. [17] investigated the connection of a beam to a steel column using a shaped memory alloy. It was observed that the hysteresis diagram is stable and has good ductility and energy dissipation. Falahian et al. [18] investigated the seismic performance of a steel frame equipped with a self-centering damper. The results showed that the proposed damper limits the residual drifts. Issa and Alam [19] evaluate steel frames equipped with Buckling Restrained Bracing (BRB), Piston Based Self Centering (PBSC) bracing, and Friction Spring Based Piston Bracing (SBPB). The results showed that frames equipped with SBPB and PBSC performed better than frames equipped with BRB. Bogdanovic et al. [20] evaluated steel structures with and without prestressed viscous dampers. The results showed that using this damper, the structural responses are reduced by 10 to 70%. Kamaludin et al. [21] evaluated three concrete frame structures equipped with three types of viscoelastic, friction, and BRB dampers. It was found that viscoelastic dampers perform better than the other two dampers. Alavi et al. [22] developed and presented a combined framework of control-structural optimization. Fathizadeh et al. [23] proposed a new system called " curved damper truss moment frame", and it was found that the proposed system satisfies the requirements of the FEMA P695 code. Aydin et al. [24] investigated the effect of soil-structure interaction on viscous dampers. Barkhordari and Tehranizadeh [25] evaluated the effect of tuned mass damper (TMD), viscous damper, friction damper, and lead core rubber bearing in damage control and seismic response of high-rise structures equipped with a concrete shear wall. Hosseinnejad et al. [26] studied the load-bearing capacity of the post-tensioned tapered steel beams by shaped memory alloy (SMA) tendons. Heydari and Gerami [27] investigated the approach of moment frames with conventional welded connections using a reversible system. Pourzangbar et al. [28] investigated the effect of different viscous damper configurations on the performance of steel frames.

Shojaeifar et al. [1] evaluated the performance of triangular added damping and stiffness (TADAS) dampers in combination with curved dampers (Curved-TADAS damper) in moment resisting steel frame (MRSF).The combination of nickel and titanium shapes memory alloys with two unique behaviours: super-elastic and shape memory. This behaviour results in them being able to withstand large strains of about 8% without creating residual strains. Also, nitinol alloy has excellent corrosion and fatigue resistance, which means that it does not need to be replaced under cyclic loads such as earthquakes.

In this study, due to the model's complexity, three reference papers [3, 7, 8] were utilized to evaluate the results of numerical modelling of SMA rods, steel dampers, and concrete shear walls equipped with steel dampers and isolator. Various numerical modelling, including material modelling, assume, behavioural models, elements used, and solution methods, different experimental results were discussed and interpreted with a numerical model. Also, the proposed system of design steel cantilever damper and SMA rod with different angles were examined.

2. SHAPE MEMORY ALLOY AND CANTILEVER DAMPER

Shaped-memory alloys are known as intelligent materials due to their unique properties. With the combination of different materials, this alloy can be produced that NiTi is one of the most widely used compounds due to its ability to withstand large strains of about 8%. The memory alloy is composed of two crystalline structures, austenite and martensite. The austenite phase is stable at high temperature, and low stress, which leads to super-elastic behaviour, and the martensite phase is stable at low temperature and high stress, which produces a shape memory behaviour. Due to its ability to change from one phase to another by applying temperature and stress, this alloy can change the residual shapes to zero.

Cantilever dampers are a type of slotted damper with one end fixed and the other end free. These dampers have deformation inside the plate and high elastic stiffness, and their geometry reduces the strain concentration due to the reduction of width to the free end. As shown in Figure 1, due to its optimized geometry, it is much more economical than other types of dampers [7].

3. NUMERICAL MODELLING AND INTERPRETATION OF RESULTS

3. 1. Numerical Modelling of Sma Rods, Validation with Experimental Results The experimental research of DesRoches et al. [3] was selected for validation on the numerical modelling. For boundary conditions, all degrees of freedom of the two ends, except for the displacement in the axial direction for the left end, was restrained. The loading was applied in a cyclic pattern in the tensile direction. Also, mesh with dimensions of 1, 2, 3, and 4 mm (corresponds to 1-SMA, 2-SMA, 3-SMA and 4-SMA numerical models) was employed. Figures 2 show the loading protocol of the SMA rod for simulation.

As shown in Figure 3, the SMA rod's stress decreases at the same strains for larger mesh models than for smaller mesh, although the results have converged in the 3-SMA and 4-SMA models. Table 1 compares the maximum numerical stress of SMA rods with experimental. In addition to the closeness of results, the solution time is also an important issue. So, the 2-SMA model with 331 seconds of solving time was selected.

3. 2. Numerical Modelling of Steel Damper, Verification with Experimental Results Experimental research of Kim et al. [7] was chosen to validate the performance of steel dampers. In the experimental specimen, the damper is connected to the rigid frame by two strong members on the left and right. For numerical modelling, boundary conditions were applied directly to the plates. Loading was applied to a reference point which restrained to the left plate by the coupling constraint. For the right plate, all degrees of freedom were fully constrained. Two types of isotropic

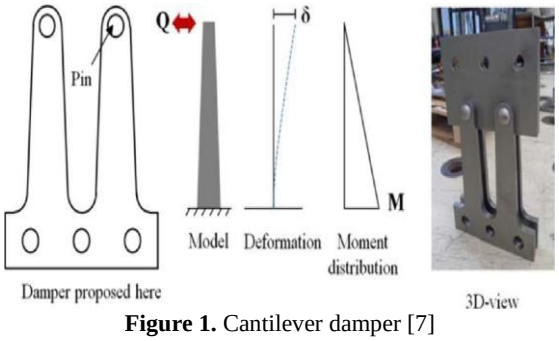

Figure 1. Cantilever damper [7]

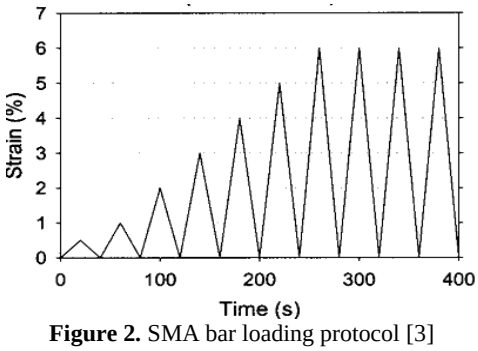

Figure 2. SMA bar loading protocol [3]

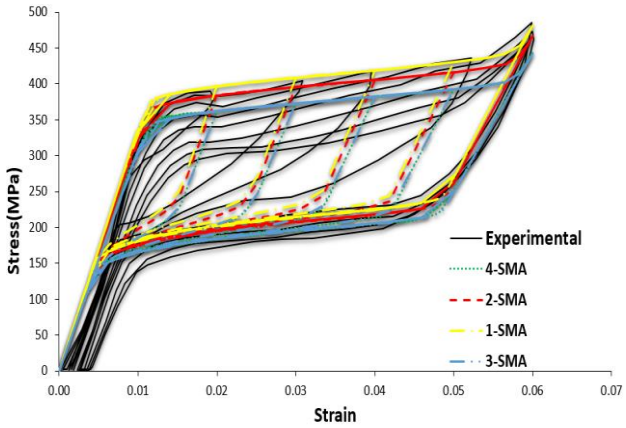

Figure 3. Comparison of stress-strain diagram of SMA rod of the experimental specimen with numerical modelling

TABLE 1. Comparison of experimental results and numerical modelling of SMA rod

Specimen		Experimental model	1-SMA	2-SMA	3-SMA	4-SMA
Maximum stress(MPa)	Drift(%2)	389	397	384	362	362
	Drift(%3)	405	409	396	373	373
	Drift(%4)	417	419	405	382	382
	Drift(%5)	436	430	416	392	392
	Drift(%6)	486	481	467	443	445
Solving time(second)		-	1650	331	117	123

and combined hardening were employed for numerical modelling. The bolts at the damper's right end were neglected in modelling and attached to the tie plate. The pins were rigidly modelled for simplification. Figures 4 and 5 show the boundary conditions and damper finite element mesh.

As shown in Figure 6, in isotropic stiffening specimens, larger hysteresis loops have been formed than in the experimental specimen. In the inelastic region, specimens constrained in the Y direction, the force-displacement diagram has revealed a steeper slope than

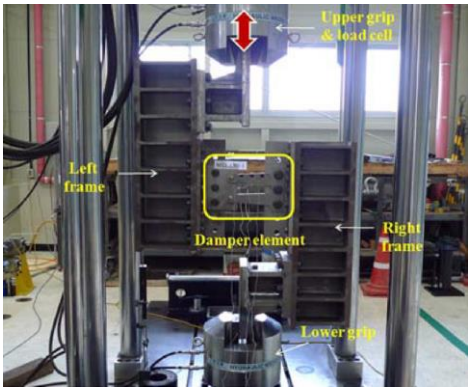

Figure 4. Steel damper boundary conditions [7]

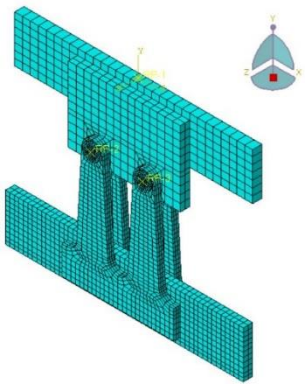

Figure 5. Damper finite element mesh

the experimental model. Nevertheless, the model combine stiffening and accessible in the Y direction fits well with the experimental findings. In Table 2, the numerical results with combined stiffening and free in the Y direction have been compared with the experimental results.

Figure 7 shows the Mises stress contours of the damper. In models released in the Y direction, stress concentration is observed at the bottom of the damper, indicating a rupture formed in this position.

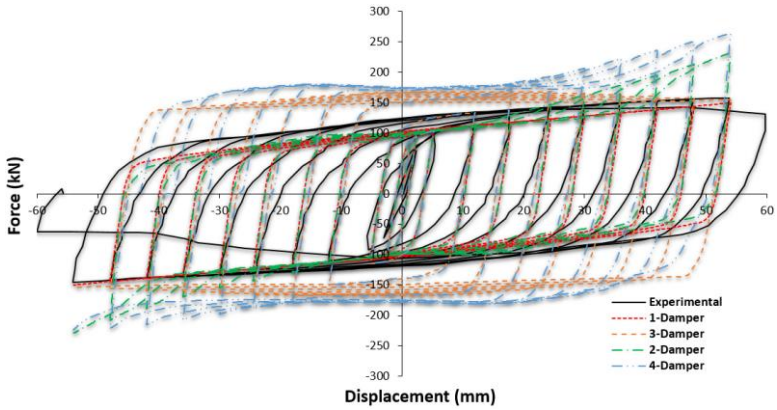

Figure 6. Comparison of force-displacement diagram of steel damper, experimental via numerical results

TABLE 2. Comparison of 1-Damper specimen with the experimental data

Specimen	1-Damper	Experimental	Difference
Yield displacement (mm)	2.5	2.63	-4.94
Yield force (kN)	96	108.40	-11.44
Initial stiffness (kN/mm)	38.4	41.22	-6.84
Second stiffness (kN)	149.68	151.30	-1.07

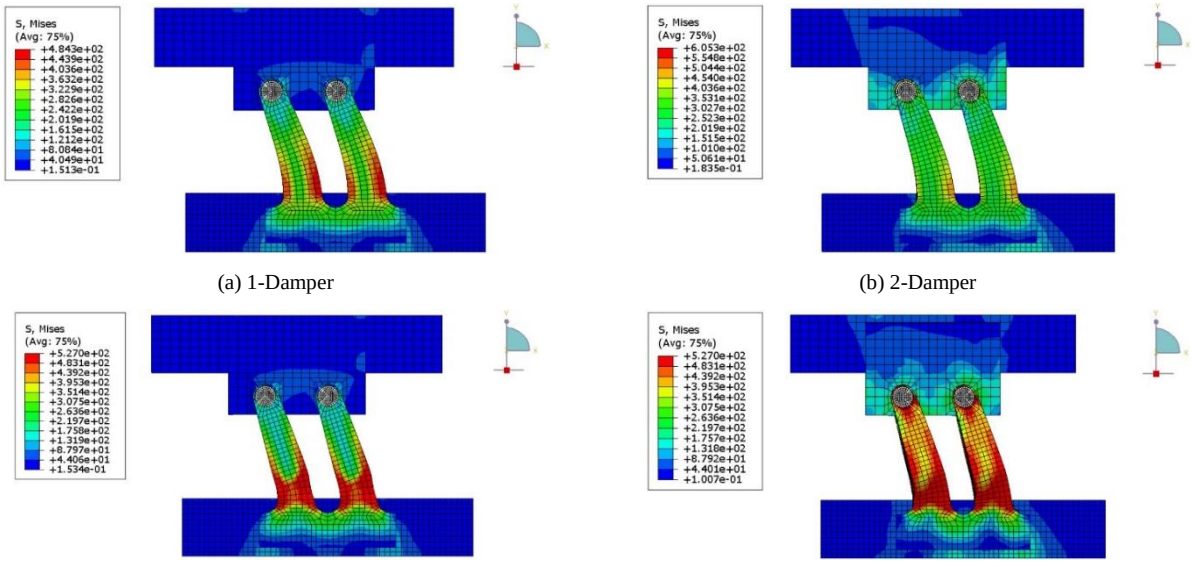

(a) 1-Damper (b) 2-Damper

(c) 3-Damper (d) 4-Damper

Figure 7. Mises stress contours in damper -54 mm displacement of (in MPa)

3. 3. Numerical Modelling of Shear Wall Equipped with Steel Damper and Seismic Isolator, Verification with Experimental Results

Experimental research of Ahn et al. [8] was selected to verify the numerical modelling of concrete shear wall equipped with an isolator and steel damper. Figure 8 shows the configuration of the wall equipped with a damper and seismic separator. Isolator rubber with different values was modelled to validate the Poisson ratio. The concrete was modelled elastic. The effect of cracking on the stiffness of the structure was considered using a cracking coefficient of 0.5. Tables 3 and 4 show the specifications of concrete and rubber materials.

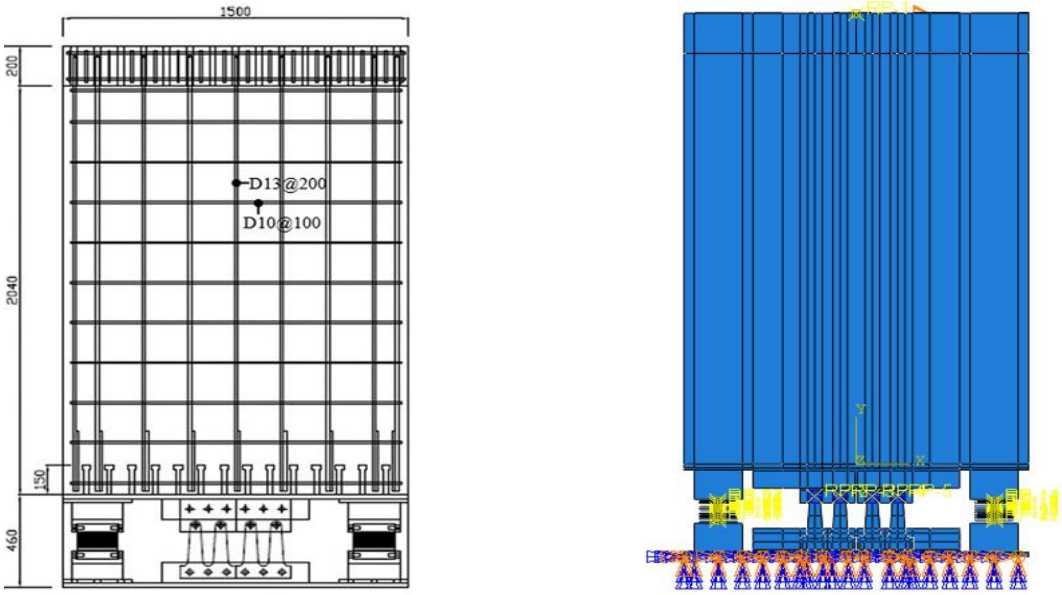

(a) Experimental modelling [8] (b) Numerical modelling

Figure 8. configuration of the wall equipped with damping and seismic separator

TABLE 3. Specifications of concrete materials

Density (kg/m^3)	2400
Specified strength (MPa)	30
Modulus of elasticity (MPa)	26154
Modulus of crack elasticity (MPa)	13077
poisson's ratio	0.15

TABLE 4. Specifications of rubber materials

Poisson's ratio	**K_H (N/mm)**	**G (N/mm^2)**	**K (N/mm^2)**	**C_{10} (N/mm^2)**	**D_1 (mm^2/N)**
0.4990	58	0.4124	206.0555	0.2062	0.0097
0.4993	58	0.4124	294.4239	0.2062	0.0068
0.4995	58	0.4124	412.2484	0.2062	0.0049

As shown in Figure 9 and Table 5, the maximum force and dissipated energy decrease by decreasing the Poisson ratio, and the residual displacement increases. The model with Poisson's ratio of 0.4993 is in good agreement with the experimental results; therefore, Poisson's ratio of 0.4993 was used to model the rubbers.

Experimental diagrams were compared with the numerical model in Figures 10 to 13 as well as Tables 6 to 8. The absence of the columns on both sides of the wall in the numerical model is responsible for differences in results of numerical models compared to experiments. There is also a distance between the hole and the pins connecting the column to the frame. Such detail has not been simulated in numerical modelling and causes the negligible pinching phenomenon in cyclic behaviour.

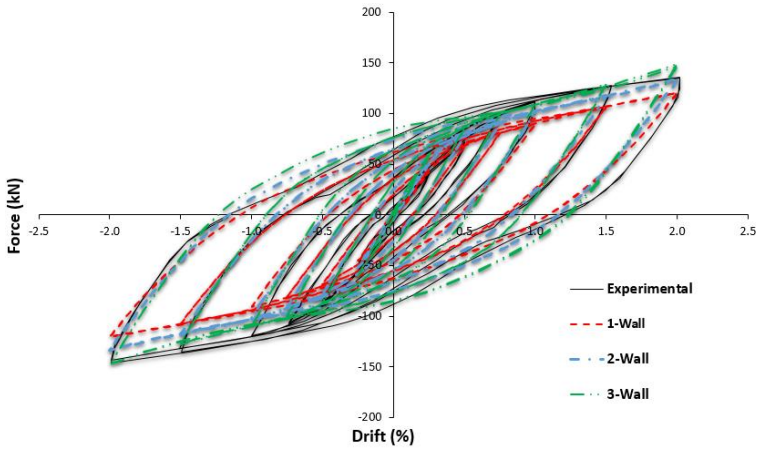

Figure 9. Comparison of force-drift diagram, experimental result vs. numerical finding

TABLE 5. Comparison of models with different Poisson ratios vs. the experimental results

Specimen	Maximum force (kN)	Maximum force difference (%)	Dissipated energy (kN.m)	Dissipated energy difference (%)	Residual displacement (mm)	Residual displacement difference (%)
Experimental	136	0	49	0	-31.59	0
1-Wall	121	-11	41.43	-15.45	-29.29	-7.28
2-Wall	134	-1.47	48.78	-0.45	-31.46	-0.41
3-Wall	149	9.5	56.84	16	-33.5	6.04

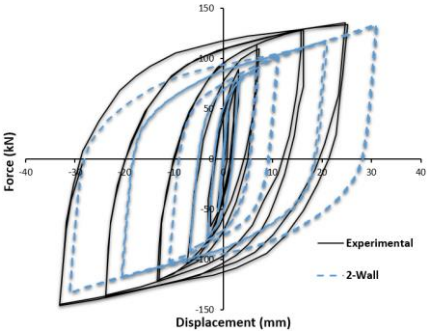

Figure 10. Dampers force-displacement diagram in 2-Wall specimen, Experimental via numerical results

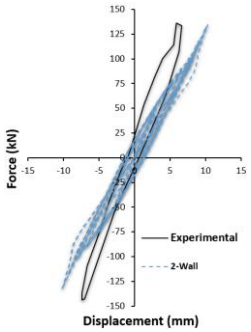

Figure 11. Wall force-displacement diagram in 2-Wall specimen, Experimental via numerical results force-displacement diagram in 2-Wall specimen, Experimental via numerical results

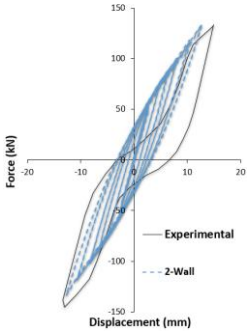

Figure 12. Wall's rigid body rotation diagram in 2-Wall specimen force-displacement diagram in 2-Wall specimen, Experimental via numerical results

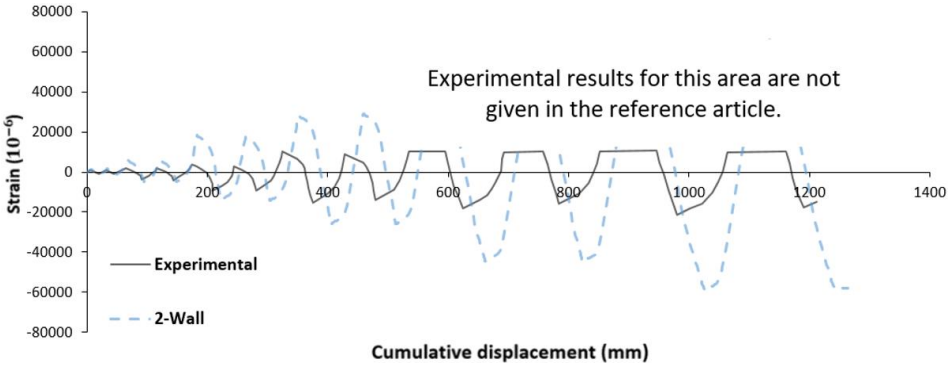

Figure 13. Comparison of damper cumulative displacement-strain diagram with numerical results in 2-Wall specimen

TABLE 6. Comparison of force-displacement results of 2-Wall specimen with the experimental model

Specimen	Maximum displacement in right side (mm)	Right maximum displacement difference (%)	Maximum displacement in left side (mm)	Left maximum displacement difference (%)
Experimental	25	0	-33	0
2-Wall	31	24	-31	-6.06

TABLE 7. Comparison of 2-Wall specimen wall deformation results with the experimental model

Specimen	Maximum displacement in right side (mm)	Right maximum displacement difference (%)	Maximum displacement in left side (mm)	Left maximum displacement difference (%)
Experimental	6.62	0	-7.38	0
2-Wall	10.32	56.89	-10.21	38.35

TABLE 8. Comparison of 2-Wall rigid body rotation result with the experimental model

Specimen	Maximum displacement in right side (mm)	Right maximum displacement difference (%)	Maximum displacement in left side (mm)	Left maximum displacement difference (%)
Experimental	14.90	0	-13.40	0
2-Wall	12.72	-14.63	-12.66	-5.52

Earthquake foreshock was taken into account in two stages. For the first step, 1%, 1.5%, and 2% of drift were applied to the specimens. 2% of drift was considered for the second stage as the main earthquake. Force-drift diagrams are presented in Figures 14 to 16.

The diagrams' difference is due to the seismic isolator's performance in the numerical model. However, the poor performance of the seismic isolator is maybe due to simplification in the simulation of elastic concrete behaviour and absence of columns in the numerical model; it has not been considered on both sides of the wall. Propagation of cracks in the concrete has caused pinching phenomena in cyclic response. There is also a difference between the hole and the pins connecting the column to the frame, which has led to differences in experimental results and numerical modelling. Figure 17 shows the seismic isolator deformation for 2% drift. Figure 18 shows the damper deformation compared to the experimental results in different drifts. As can be seen, in drift 2%, numerical deformation matches the experimental specimen. However, with increasing drift, there is a difference between the deformation of numerical models and corresponding experimental results due to high seismic isolator deformation in the numerical model compared to the experimental.

3. 4. Performance Evaluation of Shear Wall Equipped with a Damper, Seismic Isolator and Sma Rod In this study, the effect of SMA rod with angles of 30, 45, and 60 degrees on the performance of concrete shear wall equipped with steel cantilever damper and seismic isolator was also evaluated. Due to the buckling in the slender members, the rod was attached to the damper so that it was only stretched. Figure 19 reveals the SMA rod assembly with a 30-degree angle to the damper.

Figure 20 presents the force-drift diagram. Table 9 shows the comparison of the models. In the model with 2 rods at an angle of 30 degrees, the displacement of residual has the most significant decrease, and in the model with 2 rods at an angle of 60 degrees, the dissipated energy has the highest increase. The results also prove that by increasing the angle of the rod, the maximum force decreases, and the dissipated energy as well as the residual displacement increases.

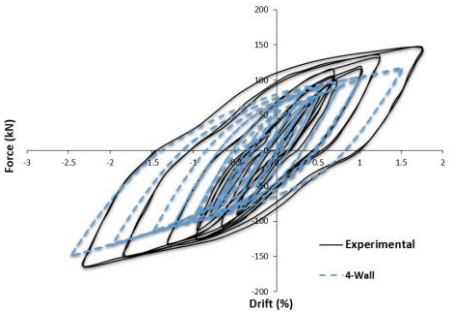

Figure 14. Comparison of force-drift diagram - experimental - via numerical model - 1% and 2% drift

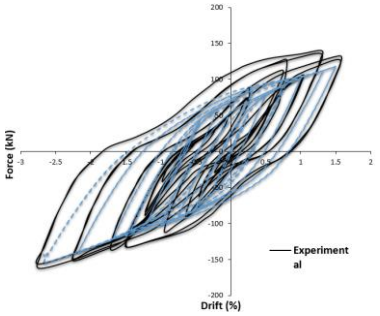

Figure 15. Comparison of force-drift diagram -experimental via numerical model - 1.5% and 2% drift

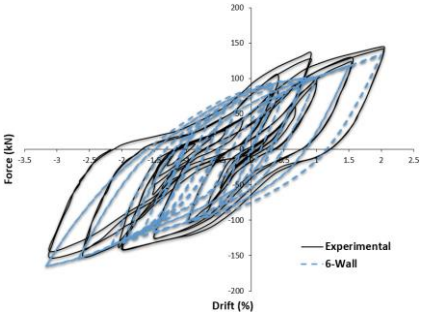

Figure 16. Force-drift diagram of the experimental via numerical model - 2% and 2% drift

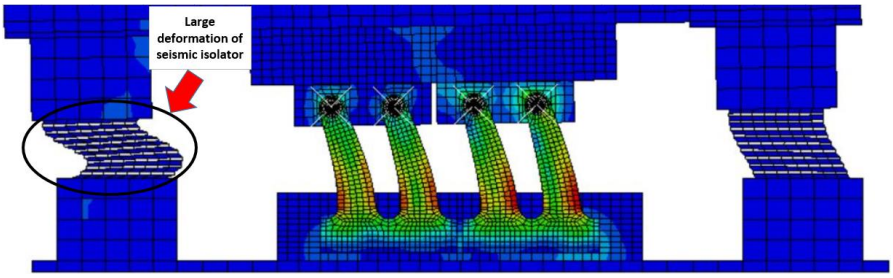

Figure 17. Deformation of the seismic isolator in the 6-Wall specimen

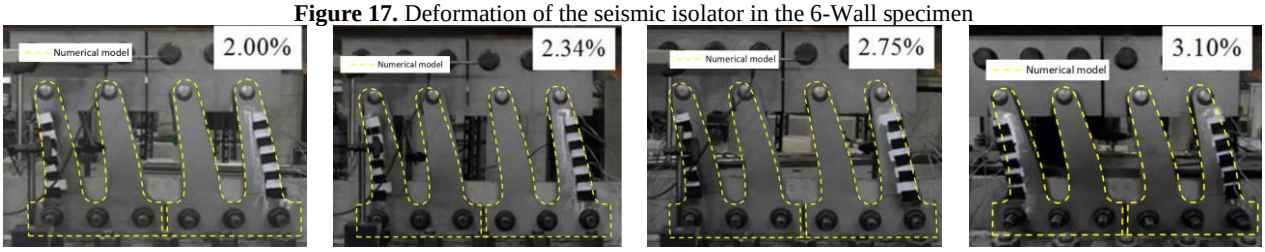

Figure 18. Comparison of experimental specimen deformation with numerical in 2% drift

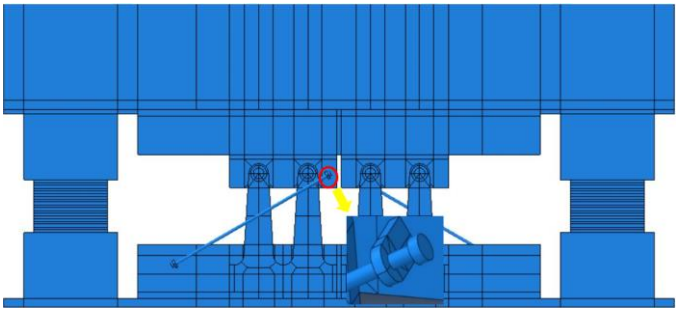

Figure 19. Specimen assembly 1-Wall-SMA

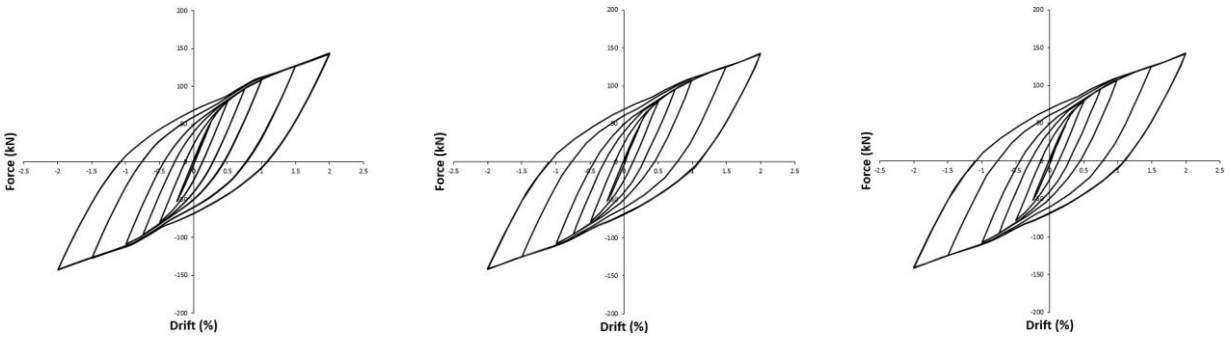

(a) specimen 1-Wall-SMA (b) specimen 2-Wall-SMA (c) specimen 3-Wall-SMA

Figure 20. Force-drift diagram of wall model equipped with steel plan damper, seismic isolator, and SMA rod

TABLE 9. Comparison of specimens with SMA rods

Specimen	Maximum force (kN)	Dissipated energy (kN.m)	Residual displacement (mm)
1-Wall-SMA	143.853	46.57	-29.28
2-Wall-SMA	142.342	47.06	-29.67
3-Wall-SMA	139.921	47.68	-30.22

Figures 21 to 23 compare a specimen's results with 2 SMA rods and a specimen without SMA rods. In the specimen with 2 SMA rods at an angle of 30 degrees compared to the specimen without SMA rods, the maximum force increases by 7.35%, the dissipated energy decreases by 4.53%, and the residual displacement decreases by 6.93%. In the specimen with 2 SMA rods at an angle of 45 degrees compared to the specimen without SMA rods, the maximum force increases by 6.23%, the dissipated energy decreases by 3.53%, and the residual displacement decreases by 5.69%. In the specimen with 2 SMA rods at an angle of 60 degrees compared to the specimen without SMA rods, the maximum force increases by 4.42%, the dissipated energy decreases by 2.26%, and the residual displacement decreases by 3.94%. The results exhibit that despite the SMA rod's positive effect, which leads to an increase in maximum force and a decrease in residual displacement, the dissipated energy decreases.

The effect of 4 SMA bars with an angle of 30 degrees on the structural system's behaviour was also examined. Figure 24 offers the assembly of 4 SMA bars with an angle of 30 degrees to the steel damper. Figure 25 demonstrates the hysteresis diagram for the specimen with 4 SMA bars, and in Figure 26 to 28**,** the results of the model without SMA bars and with 2 and 4 SMA bars are compared. Based on the findings, the maximum force

in the specimen with 4 SMA rods compared to the specimen with 2 SMA rods and without SMA rods increases by 6.38% and 14.20%, respectively, and the dissipated energy by 4.4% and 8.73%, respectively, and the residual displacement by It decreases by 7.31% and 13.73%.

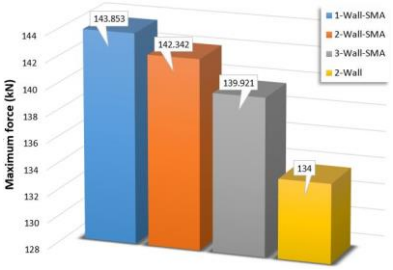

Figure 21. Comparison of maximum force for the specimen with SMA rod and without SMA rod

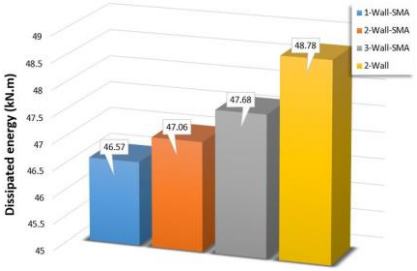

Figure 22. Comparison of dissipated energy for the specimen with SMA rod and without SMA rod

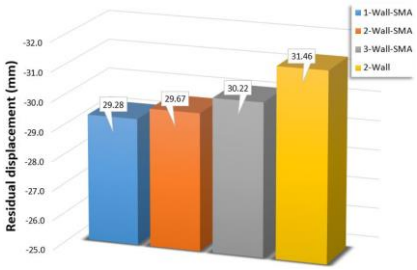

Figure 23. Comparison of residual displacement for the specimen with SMA rod and without SMA rod

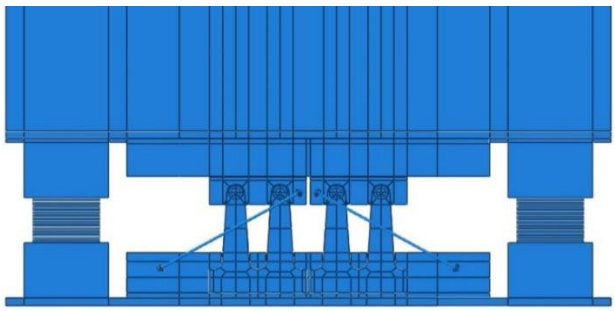

Figure 24. Specimen assembly 4-Wall-SMA

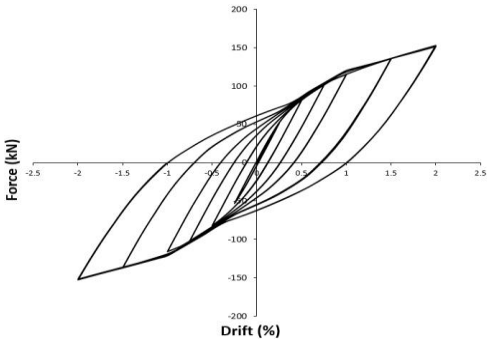

Figure 25. Force-drift diagram - 4-Wall-SMA

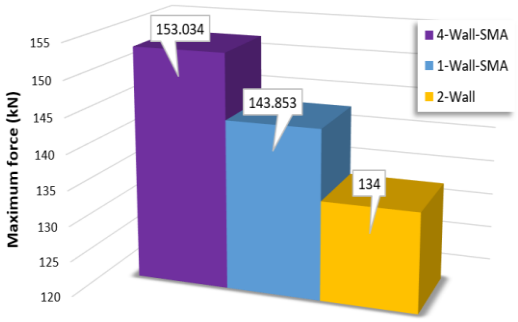

Figure 26. Comparison of maximum force for specimens with 2 and 4 SMA bars and without SMA bars

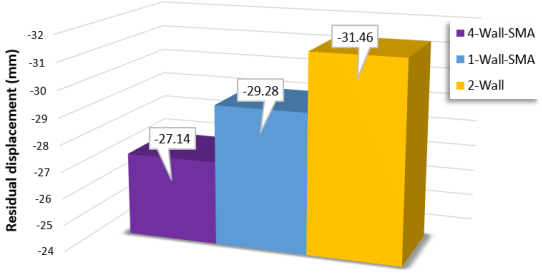

Figure 27. Comparison of residual displacements for specimens with 2 and 4 SMA bars and without SMA bars

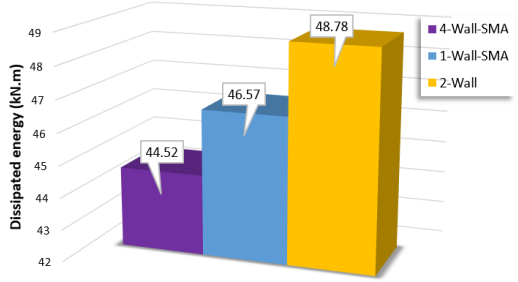

Figure 28. Comparison of dissipated energy for specimens with 2 and 4 SMA rods and without SMA rods

4. CONCLUSION

The most important findings of the present study are summarised as follows.

1. Steel dampers were modelled with isotropic, combined hardness, restrain and free in Y coordinate, respectively. Models with isotropic hardening revealed larger hysteresis loops than the experimental specimen. Moreover, in the specimens restrained in the Y direction, the force-displacement diagram had a steeper slope in the inelastic region than the experimental specimen. The model with combined hardening and release in the Y direction fits well with the experimental data.
2. Seismic isolator rubbers were modelled with Poisson's ratios of 0.4990, 0.4993, and 0.4995. The model with Poisson's ratio of 0.4993 compared well to the experimental specimen in maximum force and dissipated energy had a difference of -1.47 and -0.45%, respectively.
3. The effect of earthquake foreshock loading was simulated in two stages, including 1%, 1.5%, and 2% drift for the first and 2% drift for the second stage. The results demonstrate that the proposed model could not simulate these types of loads due to the poor performance of the seismic separator.
4. Three specimens were modelled with 30, 45, and 60-degree of SMA rod angles to investigate the SMA rod's efficiency. The results illustrated that with increasing rod angle, the maximum force decreases, and the dissipated energy and the residual displacement increased.
5. Comparing the results of specimens with SMA rods and without SMA rods showed that despite the positive effect of SMA rods to increase in the maximum force and a decrease in residual displacement, the dissipated energy had been decreased. The results also showed that in the specimen with four SMA rods compared to the sample with two SMA rods and without SMA rods, the maximum force increases by 6.38 and 14.20%, respectively, the dissipated energy by 4.4 and 8.73%, respectively, and the residual displacement decrease by 7.31 and 13.73%, respectively.

5. REFERENCES

1. Shojaeifar H., Maleki A., and Lotfollahi-Yaghin M.A., "Performance evaluation of curved-TADAS damper on seismic response of moment resisting steel frame", ***International Journal of Engineering, Transactions A: Basics***, Vol. 33, No. 1, (2020), 55-67, DOI: 10.5829/IJE.2020.33.01A.07.
2. DesRoches R. and Smith B., "Shape memory alloys in seismic resistant design and retrofit: a critical review of their potential and limitations", ***Journal of Earthquake Engineering***, Vol. 8, No. 3, (2004), 415-429, DOI: https://doi.org/10.1080/13632460409350495.
3. DesRoches R., McCormick J., and Delemont M., "Cyclic Properties of Superelastic Shape Memory Alloy Wires and Bars", ***Journal of Structural Engineering***, Vol. 130, No. 1, (2004), 38-46, DOI: 10.1061/(ASCE)0733-9445(2004)130:1(38).
4. Sayyaadi H. and Zakerzadeh M., "Nonlinear Analysis of a Flexible Beam Actuated by a Couple of Active SMA Wire Actuators", ***International Journal of Engineering, Transactions A: Basics***, Vol. 25, No. 3, (2012), 249-264, DOI: 10.5829/idosi.ije.2012.25.03a.07.
5. Kim Y., Ahn T., Kim H., and Jang D., "Development of new steel damper for seismic retrofit of existing structures", ***in Proceedings of 15th world conference on earthquake engineering***, (2012).
6. Lu X., Mao Y., Chen Y., Liu J., and Zhou Y., "New structural system for earthquake resilient design", ***Journal of Earthquake and Tsunami***, Vol. 7, No. 03, (2013), 1350013, DOI: https://doi.org/10.1142/S1793431113500139.
7. Kim Y.J., Ahn T.-S., Bae J.-H., and Oh S.-H., "Experimental study of using cantilever type steel plates for passive energy dissipation", ***International Journal of Steel Structures***, Vol. 16, No. 3, (2016), 959-974, DOI: https://doi.org/10.1007/s13296-014-0121-6.
8. Ahn H.-J., Kim Y.-J., Bae J.-H., and Jung I.-Y., "Cyclic loading test of wall damping system with steel dampers", ***Advances in Structural Engineering***, Vol. 19, No. 8, (2016), 1262-1274, DOI: 10.1177/1369433216642068.
9. Naeem A., Eldin M.N., Kim J., and Kim J., "Seismic performance evaluation of a structure retrofitted using steel slit dampers with shape memory alloy bars", ***International Journal of Steel Structures***, Vol. 17, No. 4, (2017), 1627-1638, DOI: 10.1007/s13296-017-1227-4.
10. Cortés-Puentes W.L. and Palermo D., "SMA tension brace for retrofitting concrete shear walls", ***Engineering Structures,*** Vol. 140, (2017), 177-188, DOI: https://doi.org/10.1016/j.engstruct.2017.02.045.
11. Liu Q. and Jiang H., "Experimental study on a new type of earthquake resilient shear wall", ***Earthquake Engineering & Structural Dynamics***, Vol. 46, No. 14, (2017), 2479-2497, DOI: 10.1002/eqe.2914.
12. Liu Q. and Jiang H., "Study on a new type of earthquake resilient shear wall", ***in Proceedings of the 16th World Conference on Earthquake Engineering***, (2017).
13. Chen C., Xiao R., Lu X., and Chen Y., "Study on the shear wall structure with combined form of replaceable devices", ***Advances in Structural Engineering***, Vol. 21, No. 9, (2018), 1327-1348, DOI: 10.1177/1369433217742525.
14. Cortés-Puentes W.L. and Palermo D., "Seismic Retrofit of Concrete Shear Walls with SMA Tension Braces", ***Journal of Structural Engineering***, Vol. 144, No. 2, (2018), 04017200, DOI: doi:10.1061/(ASCE)ST.1943-541X.0001936.
15. Wang B. and Zhu S., "Seismic behavior of self-centering reinforced concrete wall enabled by superelastic shape memory alloy bars", ***Bulletin of Earthquake Engineering***, Vol. 16, No. 1, (2018), 479-502, DOI: 10.1007/s10518-017-0213-8.
16. NourEldin M., Naeem A., and Kim J., "Life-cycle cost evaluation of steel structures retrofitted with steel slit damper and shape memory alloy–based hybrid damper", ***Advances in Structural Engineering***, Vol. 22, No. 1, (2019), 3-16, DOI: 10.1177/1369433218773487.
17. Wang W., Fang C., Feng W., Ricles J., Sause R., and Chen Y., "SMA-based low-damage solution for self-centering steel and composite beam-to-column connections", ***Journal of Structural Engineering***, Vol. 146, No. 6, (2020), 04020092, DOI: https://doi.org/10.1061/(ASCE)ST.1943-541X.0002649.

18. Falahian A., Asadi P., Riahi H.T., and Haghy M., "Seismic performance assessment of steel frames with shape-memory alloy wire-based dampers", ***The Structural Design of Tall and Special Buildings***, Vol. 29, No. 16, (2020), e1797, DOI: https://doi.org/10.1002/tal.1797.
19. Issa A. and Alam M.S., "Comparative seismic fragility assessment of buckling restrained and self-centering (friction spring and SMA) braced frames", ***Smart Materials and Structures***, Vol. 29, No. 5, (2020), 055029, DOI: https://doi.org/10.1088/1361-665X/ab7858.
20. Bogdanovic A., Rakicevic Z., and Noroozinejad Farsangi E., "Shake table tests and numerical investigation of a resilient damping device for seismic response control of building structures", ***Structural Control and Health Monitoring***, Vol. 26, No. 11, (2019), e2443, DOI: https://doi.org/10.1002/stc.2443.
21. Kamaludin P.N.C., Kassem M.M., Farsangi E.N., Nazri F.M., and Yamaguchi E., "Seismic resilience evaluation of RC-MRFs equipped with passive damping devices", ***Earthquakes and Structures***, Vol. 18, No. 3, (2020), 391-405, DOI: https://doi.org/10.12989/eas.2020.18.3.391
22. Alavi A., Dolatabadi M., Mashhadi J., and Farsangi E.N., "Simultaneous optimization approach for combined control–structural design versus the conventional sequential optimization method", ***Structural and Multidisciplinary Optimization***, Vol. 63, No. 3, (2021), 1367-1383, DOI: https://doi.org/10.1007/s00158-020-02765-3.
23. Fathizadeh S.F., Dehghani S., Yang T.Y., Noroozinejad Farsangi E., Vosoughi A.R., Hajirasouliha I., Takewaki I., Málaga-Chuquitaype C., and Varum H., "Trade-off Pareto optimum design of an innovative curved damper truss moment frame considering structural and non-structural objectives", ***Structures***, Vol. 28, (2020), 1338-1353, DOI: https://doi.org/10.1016/j.istruc.2020.09.060.
24. Aydin E., Ozturk B., Bogdanovic A., and Farsangi E.N., "Influence of soil-structure interaction (SSI) on optimal design of passive damping devices", ***Structures***, Vol. 28, (2020), 847-862, DOI: https://doi.org/10.1016/j.istruc.2020.09.028.
25. Barkhordari M.S. and Tehranizadeh M., "Ranking Passive Seismic Control Systems by Their Effectiveness in Reducing Responses of High-Rise Buildings with Concrete Shear Walls Using Multiple-Criteria Decision Making", ***International Journal of Engineering, Transactions B: Applications***, Vol. 33, No. 8, (2020), 1479-1490, DOI: 10.5829/ije.2020.33.08b.06.
26. Hosseinnejad H., Lotfollahi -Yaghin M., Hosseinzadeh Y., and Maleki A., "Numerical Investigation of Response of the Post-Tensioned Tapered Steel Beams with Shape Memory Alloy Tendons", ***International Journal of Engineering, Transactions A: Basics***, Vol. 34, No. 4, (2021), 782-792, DOI: 10.5829/ije.2021.34.04a.04.
27. Heydari. T A.M. and Gerami M., "Multi-stage Performance Upgrade of Steel Moment Frames by Post-tension Connections", ***International Journal of Engineering, Transactions B: Applications***, Vol. 34, No. 5, (2021), 1132-1144, DOI: 10.5829/ije.2021.34.05b.07.
28. Pourzangbar A., Vaezi M., Mousavi S.M., and Saber A., "Effects of Brace-viscous Damper System on the Dynamic Response of Steel Frames", ***International Journal of Engineering, Transactions B: Applications***, Vol. 33, No. 5, (2020), 720-731, DOI: 10.5829/ije.2020.33.05b.02.

Persian Abstract

چکیده

آلیاژ حافظه‌دار شکلی(SMA) دارای قابلیت منحصر به فرد رفتار ابر کشسان و حافظه شکلی است؛ این رفتار باعث می‌شود تا در کرنش‌های بزرگ، آلیاژ حافظه‌دار شکلی کرنش پسماندی در حدود صفر داشته باشد. در کنار این مزیت، رفتار تنش- کرنش آلیاژ حافظه‌دار شکلی در رفتار ابرکشسان شکل پرچم گونه دارد و قابلیت استهلاک انرژی زیادی نداشته و قابل جایگزین شدن با میراگر فلزی نمی باشد. برای جبران ضعف ذکر شده در میراگرهای فلزی، در تحقیق حاضر عملکرد کاربرد هم زمان این دو عضو در دیوار برشی بتن مسلح مورد بررسی قرار گرفته است و عملکرد میراگر ترکیبی (میراگر طره‌ای فولادی و میله SMA) به عنوان یک سیستم لرزه‌ای نوآورانه مورد بررسی قرار گرفته است. مدلسازی عددی در نرم افزار آباکوس انجام شده است. در این خصوص به صحت سنجی کامل ۳ مدل آزمایشگاهی پرداخته شده است. به منظور داشتن درک جامع از صحت نتایج مدلسازی عددی، در قسمت صحت سنجی تنها به مقایسه رفتار نیرو-تغییرمکان اکتفا نشده است وتاریخچه کرنشها و تغییر مکان های قسمت های مختلف سازه حاصل از مدل آزمایشگاهی با مدل عددی مورد مقایسه انتقادی قرار گرفته است. همچنین جنبه‌های گوناگون مدلسازی عددی اعم از فرضیات مدلسازی مصالح، مدل‌های رفتاری، المان‌های مورد استفاده و روش‌های حل در مقایسه با نتایج آزمایشگاهی مورد بحث و تفسیر قرار گرفته است. نتایج نشان دادند با افزایش زاویه میله SMA نیروی حداکثر کاهش و جابه‌جایی پسماند و انرژی مستهلک شده افزایش می‌یابد. علاوه براین، مقایسه نتایج نمونه بدون میله SMA و نمونه با میله SMA نشان دادند برخلاف تاثیر مثبت میله SMA که منجر به افزایش نیرو حداکثر و کاهش جابه‌جایی پسماند می‌شود، انرژی مستهلک شده کاهش می‌یابد.